Eur Biophys J (2001) 30: 295–303
DOI 10.1007/s002490100134

ARTICLE

**Kishani M. Ranatunga · Richard J. Law
Graham R. Smith · Mark S. P. Sansom**

Electrostatics studies and molecular dynamics simulations of a homology model of the *Shaker* K^+ channel pore

Received: 19 October 2000 / Revised version: 19 December 2000 / Accepted: 20 December 2000 / Published online: 13 March 2001

Abstract A homology model of the pore domain of the *Shaker* K^+ channel has been constructed using a bacterial K^+ channel, KcsA, as a template structure. The model is in agreement with mutagenesis and sequence variability data. A number of structural features are conserved between the two channels, including a ring of tryptophan sidechains on the outer surface of the pore domain at the extracellular end of the helix bundle, and rings of acidic sidechains close to the extracellular mouth of the channel. One of these rings, that formed by four Asp447 sidechains at the mouth of the *Shaker* pore, is shown by pK_A calculations to be incompletely ionized at neutral pH. The potential energy profile for a K^+ ion moved along the central axis of the *Shaker* pore domain model selectivity filter reveals a shallow well, the depth of which is modulated by the ionization state of the Asp447 ring. This is more consistent with the high cation flux exhibited by the channel in its conductance value of 19 pS.

Keywords Potassium channel · *Shaker* · pK_A calculation · Electrostatics · Molecular dynamics

K. M. Ranatunga[1] · R. J. Law · G. R. Smith[2]
M. S. P. Sansom (✉)
Laboratory of Molecular Biophysics,
The Rex Richards Building,
Department of Biochemistry, University of Oxford,
South Parks Road, Oxford, OX1 3QU, UK
E-mail: mark@biop.ox.ac.uk
Tel.: +44-1865-275371
Fax: +44-1865-275182

Present addresses:
[1] Biophysics Section, Blackett Laboratory,
Imperial College of Science, Technology and Medicine,
Prince Consort Road, London, SW7 2BZ, UK

[2] Biomolecular Modelling Laboratory,
Imperial Cancer Research Fund,
44 Lincoln's Inn Fields, London, WC2A 3PX, UK

Introduction

Ion channels enable the diffusional flow of selected ions across cell membranes. Potassium channels are widespread, being found in membranes of some viruses (Plugge et al. 2000) and of bacteria (MacKinnon et al. 1998), plants (Schachtman 2000) and animals. In excitable cells of animal nervous systems, K^+ channels play an important role both in generating and regulating action potentials (Hille 1992). Given their ubiquity and diverse physiological roles, it is important to be able to relate the function of K^+ channels to their molecular structure.

A bacterial K^+ channel, KcsA, has been described in *Streptomyces lividans* (Schrempf et al. 1995). It resembles other K^+ channels in its ion selectivity and sensitivity to K^+ channel blocking compounds such as tetraethylammonium (TEA) (Heginbotham et al. 1999; Meuser et al. 1999). The X-ray structure of this channel has been determined (Doyle et al. 1998) to 3.2 Å resolution. It has been the subject of a number of experimental (Meuser et al. 1999; Perozo et al. 1999, 2000) and computational (Allen et al. 2000; Åqvist and Luzhkov 2000; Bernèche and Roux 2000; Biggin et al. 2001; Guidoni et al. 1999, 2000; Ranatunga et al. 2001; Roux and MacKinnon 1999; Sansom et al. 2000; Shrivastava and Sansom 2000; Tieleman et al. 2001a) studies to elucidate the relationship between its structure and its biological function. However, the X-ray structure of a mammalian K^+ channel has yet to be determined. An alternative approach is to use the KcsA structure as a template upon which to base homology (comparative) models of mammalian K^+ channels (Capener et al. 2000; Thompson et al. 2000).

The *Shaker* potassium channel of the fruit-fly *Drosphilia melanogaster* was the first K^+ channel to be cloned (Tempel et al. 1987) and is one of the most extensively studied of all ion channels. It provides a paradigm for the large class of voltage-gated K^+ (K_v) channels. In response to changes in the potential

difference across the membrane, K_v channels open and close to regulate the flow of K^+ ions across a membrane. In so doing they control a variety of processes, including neuronal excitability. There is a marked degree of sequence identity between KcsA and the pore-lining regions of K_v channels (Doyle et al. 1998), which makes homology modelling particularly favourable.

We present here a model of the *Shaker* pore built using KcsA as a template structure. The model has been refined by determination of its likely ionization state. Calculation of the potential energy of interaction between a K^+ ion and the (solvated) channel is used to explore the effect of ionization state of key sidechains on channel function.

Methods

Sequence alignment and secondary structure prediction

Sequence alignment was performed using the program AMPS (Barton 1990), employing the blosum62 matrix with a gap penalty of 4. The sequences were that of KcsA (residues 23–118), corresponding to the truncated sequence visible in the X-ray structure (pdb code 1BL8), and the *Shaker* A sequence (PIR accession code S00479) truncated at both ends to include only the putative S5 to S6 region. The extents of the S5 and S6 transmembrane (TM) helices were determined from the most generous assignment of helicity deduced from TM helix predictions. The latter were performed using DAS [http://www.biokemi.su.se/~server/DAS (Cserzo et al. 1997)], TMAP [http://www.embl-heidelberg.de/tmap/tmap_info.html (Persson and Argos 1994, 1997)], PHDhtm [http://www.embl-heidelberg.de/predictprotein (Rost et al. 1995, 1996)] and TopPred2 [http://www.biokemi.su.se/~server/toppred2 (von Heijne 1992)], and verified by MD studies on isolated S5 and S6 helices embedded in a POPC bilayer (Shrivastava et al. 2000).

Homology modelling

Homology models were produced from the sequence alignment using Modeller4 (Sanchez and Sali 1997), with additional restraints to preserve predicted TM helical regions and the four-fold symmetry of the pore. Thus, the M1, P and M2 helical regions were restrained to adopt an α-helical conformation, and the non-crystallographic four-fold symmetry present in the KcsA structure was enforced in the *Shaker* models. From an ensemble of 25 structures generated by Modeller, the five that scored best with respect to satisfaction of the restraints used in model generation were selected. These five models were very similar to one another. One of the five models was selected that ranked highly over several tests of stereochemistry [Procheck (Laskowski et al. 1993), Quanta (Momany and Rone 1992) and Whatif (Rodriguez et al. 1998; Vriend 1990)], as well as being the closest to the KcsA structure template used in Modeller (i.e. this model was ranked most highly by Modeller). We note that the Cα RMSDs of each of the five models versus KcsA was ca. 1.4 Å, and that the Cα RMSDs between all pairs of the five models were ca. 0.2 Å. Hence these five structures represent a very "tight" cluster of models, and thus differences between the five models are unlikely to be a significant source of error in subsequent calculations. On the basis of previous experience in pK_A calculations for ion channel models (Adcock et al. 1998, 2000; Ranatunga et al. 1998; Ranatunga et al. 1999; Tieleman et al. 1998), and taking into account the relatively low resolution of the template structure (3.2 Å), it was judged sufficient to analyse just a single representative model. One would expect as little difference between conclusions drawn from such analyses as between MD snapshots of the "same" structure (Ranatunga et al. 1998). This model was energy minimized (in vacuo), using Charmm24, first with 2000 steps of ABNR (adopted basis Newton-Raphson) with all backbone atoms fixed and then with 2000 steps of ABNR with only the Cα atoms fixed so as to allow some relaxation of the protein backbone and sidechains.

ASA analysis

Sequence variability in the S5 and S6 helix regions of multiple alignments of 14 different K_v channels was performed using Perscan (Donnelly et al. 1993). The sequence variability (defined as the number of different amino acids at a given position in the sequence alignment) of each residue (i.e. each position in the alignment) was plotted against the fractional solvent accessible area of the corresponding residue in the KcsA structure (calculated using Quanta, using a probe radius of 1.4 Å). Linear regression yielded the correlation coefficient between sequence variability and fractional accessible surface area for each helix. This correlation coefficient was calculated for different shifts of the K_v channel multiple alignment relative to the KcsA sequence.

pK_A calculations

The calculation of sidechain ionization states used established methods (Bashford and Karplus 1990; Yang et al. 1993). Its application to ion channel models has been described in detail elsewhere (Adcock et al. 1998; Ranatunga et al. 1999, 2001). It is based on numerical solution [using UHBD (Davis et al. 1991)] of the linearized Poisson-Boltzmann equation to calculate the difference between: (1) the change in electrostatic free energy upon protonation of the sidechain of an amino acid isolated in solution (for which the pK_A is the model, i.e. experimental, value); and (2) the corresponding change in free energy for the same sidechain within a protein. This difference is evaluated from a sum of the free energy of solvation of the sidechain into its dielectric environment (the Born energy) and the free energy of interaction of the sidechain with the background of partial charges due to the polypeptide chain and the other (un-ionized) sidechains in the protein (the "back" energy). This yields an "intrinsic" pK_A for a sidechain in the protein. Then pairwise interactions between the different ionizable residues in the protein are estimated, and used to evaluate a Boltzmann-weighted sum over all protonation states of these sidechains (via a Monte-Carlo routine), thus yielding titration curves for each ionizable sidechain in a protein molecule. In these calculations, the protein is represented at atomistic level with atomic radii and partial charges [using the Charmm 22 parameter set (Momany and Rone 1992)] and is embedded in a low dielectric bilayer mimic. The latter is composed of a slab of overlapping methane spheres 30 Å in thickness. The protein and "bilayer" are assigned a relative permittivity of 4 and the remaining space a value of 80 and an ionic strength of 100 mM KCl. UHBD5.1 was employed for all electrostatics calculation with a two-grid focusing protocol.

Molecular dynamics

Molecular dynamics (MD) simulations employed the *Shaker* pore model solvated with 2662 modified TIP3P water molecules so as to fill the central pore and to provide "caps" of water molecules at the extracellular and intracellular mouths of the channel. Potential energy profiles for ion/protein and ion/water interactions were calculated from brief MD simulations in which a K^+ ion was placed at successive 1 Å positions along the pore (z) axis of the solvated model [see Ranatunga et al. (1998); Ranatunga et al. (2001); Smith and Sansom (1997) for details]. Harmonic restraints (force constant of 10 kcal mol^{-1} Å^{-2}) were applied to the z-position of the ion and the system was energy minimized (3000 steps ABNR), heated (to 300 K for 6 ps) and equilibrated (9 ps). Shift functions acting between 13 Å and 14 Å were employed to

truncate long-range interactions. Harmonic restraints were applied to the Cα atoms [see Ranatunga et al. (2001) for details] with force constants corresponding to the mean square fluctuations of the corresponding atoms of KcsA in a full bilayer simulation. A miscellaneous mean field potential (MMFP) cylindrical restraint was applied to the water molecules in the caps at either end of the channel model. The potential energies of ion/protein and ion/water interactions were averaged over the 9 ps period. MD simulations used CHARMm24 (Brooks et al. 1983).

At some z-position of the K^+ ion, energy fluctuations were found to be too high to proceed in the heating stage. In these cases, the model was subjected to a further 4000 steps ABNR minimization before heating. If this still did not resolve the problem, a further 1000–5000 steps ABNR was performed with our calculated Cα harmonic restraints. Energy fluctuations were still too large at some positions, leading to "missing" points. These energy violations are due to the extreme constriction of the channels at these points (particularly in the intracellular "gate" region), suggesting that an ion would find it particularly unfavourable to remain in that position. Of course, we realize that in this region of the channel model the extreme constriction of the pore may simply reflect inaccuracies in the model, as discussed below.

All calculations were performed on either Silicon Graphics O2 workstations or a Silicon Graphics Origin2000. Structures were examined with Rasmol and Quanta, and structural diagrams generated using Molscript (Kraulis 1991) and Raster3D (Merritt and Bacon 1997).

Results

Building the *Shaker* pore model

The most important factor in determining the quality of a homology model is the sequence alignment between the protein to be modelled and the template protein. The alignment between the *Shaker* pore and KcsA shows a percentage identity of 34% over the whole S5-P-S6 region. There is particularly strong sequence conservation within the pore helix and selectivity filter region and no gaps or insertions are needed in the alignment (Fig. 1). The secondary structure predictions on the *Shaker* sequence are encouraging in that they agree well with the observed TM helical regions in the KcsA structure. Combined with the functional homology between the two proteins (i.e. they are both K^+ channels) (MacKinnon et al. 1998), this justifies an attempt to homology model the *Shaker* pore domain.

Evaluation of the model

The model was compared against a large body of Cys-scanning and other mutagenesis data drawn from the literature [see e.g. Kerr and Sansom (1997) for a summary of some of this data] and found to be compatible with it, as suggested by Doyle et al. (1998). We have also evaluated the *Shaker* homology model by analysing the distribution of conserved and variable residues in the sequences of K_v channels in terms of their location in the *Shaker* model. For some time it has been suggested that, on average, the more exposed residues in membrane proteins show a lesser degree of sequence conservation than do buried residues (Komiya et al. 1987).

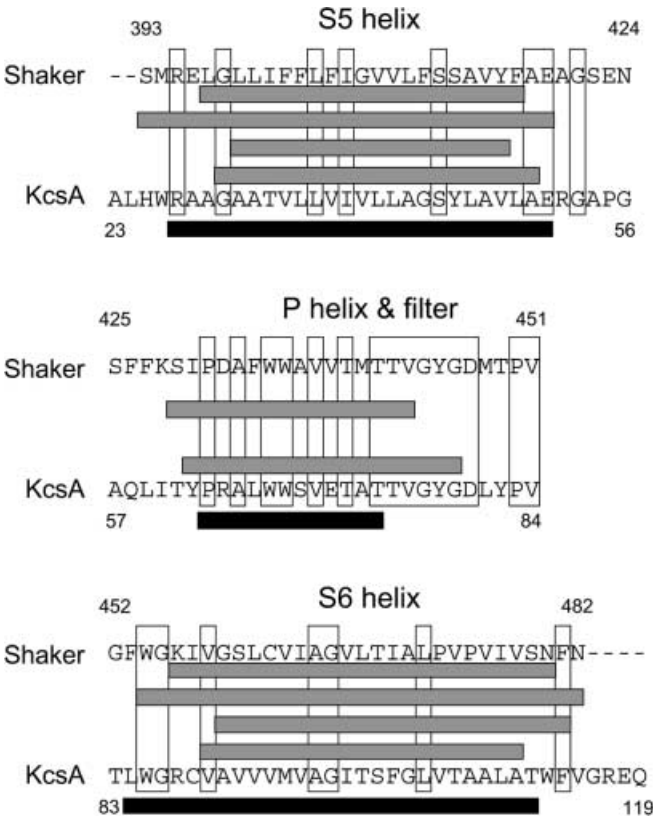

Fig. 1 Sequence alignment between *Shaker* (residues 393–482) and KcsA (residues 23–119), with identical residues *boxed*. TM helix predictions for *Shaker* are shown as *grey bars* (predictions using, from top to bottom, DAS, TMAP, PHDhtm and TopPred2), whilst the extents of the M1, P and M2 helices as defined by the crystal structure of KcsA are shown as *black bars*

Furthermore, as the S5-P-S6 core of K_v channels is believed to be "older" (in evolutionary terms) than the surrounding S1 to S4 helices (http://nt-salkoff.wustl.edu), one might anticipate a "gradient" of sequence conservation from the core of the molecule towards its peripheral TM helices (Durell et al. 1998). Accordingly, the correlation between relative surface accessibility of a residue (in KcsA) versus the sequence variability of the residue position in a K_v multiple alignment was evaluated for different shifts of the *Shaker* (K_v) alignment relative to the KcsA sequence (the "zero shift" alignment being that in Fig. 1). The results of this analysis (Fig. 2) reveal a periodicity in the correlation coefficient versus alignment shift for both the S5 and S6 helices. This is expected if these TM segments indeed adopt an α-helical conformation as predicted. Furthermore, for the TM helices considered together there is a strong maximum corresponding to the zero shift in the alignment, and thus the zero shift represents the global optimal alignment. This confirms that the alignment given in Fig. 1 maximizes the exposure of variable residue positions on the surface of the *Shaker* channel domain model. Even though the $(S5\text{-}P\text{-}S6)_4$ core is believed to be surrounded by the S1 to S4 helices in the intact channel, this analysis supports the idea that the

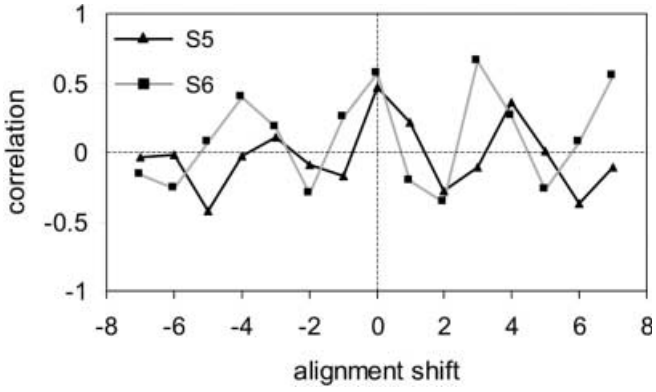

Fig. 2 Correlation coefficient (for relative accessible surface area versus residue variability in a K_v sequence alignment variability; see main text for details) as a function of shift (in residues) of the alignment of *Shaker* S5 (*triangles and black lines*) and of S6 (*squares and grey lines*) helix sequences versus those of KcsA. A shift of zero in the alignment corresponds to the alignments shown in Fig. 1

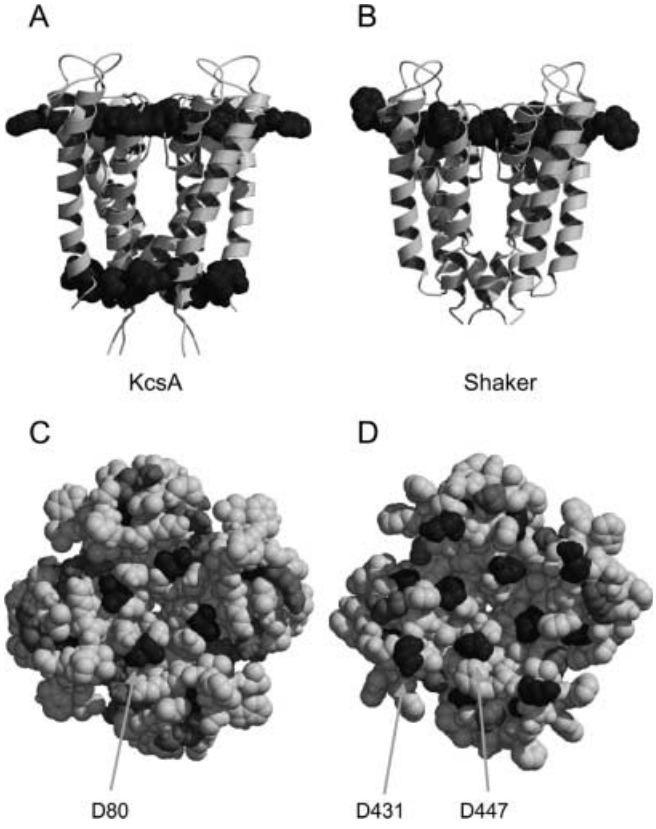

Fig. 3 **A**, **B** KcsA and the *Shaker* pore model displayed in ribbon format (*pale grey*) with their tryptophan sidechains in space-filling format in *dark grey*. **C**, **D** KcsA and the *Shaker* pore model displayed in space-filling format and viewed from the extracellular face. Acidic residues are in *dark grey*, basic residues in *mid-grey* and all other residues in *pale grey*. The key rings of acidic sidechains at the pore mouths are indicated

channel-forming core is highly conserved. In particular, protein/protein contacts within this core are conserved. This is to be expected if the structural integrity of the core domain is essential to channel function, and if the KcsA structure is the correct template for modelling this domain.

Some key structural features are conserved between the KcsA structure and the *Shaker* model. For example, the two structures exhibit similar distributions of tryptophan residues (Fig. 3A, B). In both cases there is a pronounced band of tryptophan sidechains at the extracellular end of the molecule. In part this corresponds to the "aromatic cuff" that has been suggested to confer rigidity to the selectivity filter region and hence influence the selectivity properties of the channel (Doyle et al. 1998). However, the band of tryptophan sidechains on the outer surface of both structures may also play a role in protein stability. It has long been noted that integral membrane proteins tend to have bands of tryptophan sidechains corresponding to the location of the water/lipid headgroup interface (Yau et al. 1998). Of course, in the intact *Shaker* protein these tryptophan sidechains will probably be buried by the surrounding S1 to S4 helices.

One may have less confidence in the *Shaker* model in regions of lower sequence similarity. One such region is the loop between the S5 helix and the pore (P) helix [corresponding to the "turret" in KcsA (Doyle et al. 1998)]. Pro55, which forms part of the turret loop in KcsA, is not conserved in *Shaker*, which may imply a different secondary structure in the *Shaker* loop. Indeed, a recent study based on estimated surface charge potentials (Elinder and Århem 1999) of this region for a number of K_v channels suggests that the N-terminal end of this loop forms a short α-helix lying parallel to the membrane surface near to the voltage-sensing S4 helix. This is consistent with experimental evidence that residues within this region influence gating (Frankenhaeuser and Hodgkin 1957). However, we have elected to start with a rather more conservative model of *Shaker* (i.e. close to KcsA in structure) and have not attempted to include this putative helix.

The Pro-Val-Pro (473–475) sequence motif in the S6 helix of *Shaker* is a conserved motif of K_v channels. The two Pro residues may confer a degree of hinge-bending flexibility on the S6 helix (Kerr et al. 1996; Sansom and Weinstein 2000; Shrivastava et al. 2000; Tieleman et al. 2001b). Intriguingly, the central Val474 of *Shaker* S6 aligns with Thr107 of KcsA M2. The latter residue is at the bottom of the aqueous cavity of KcsA and its only polar constituent. Blocker protection studies on the S6 helix of *Shaker* (Camino et al. 2000) suggest that there may be a kink at the Pro-Val-Pro region, leading to a wider intracellular mouth than would otherwise be expected. Taken together, these results suggest that the conformation of S6 may change during gating of the channel. As we have not attempted to place the kink in the S6 helix in the current model of the *Shaker* pore, we would suggest that our model corresponds more closely to a *closed* state of the channel. This is in agreement with the current belief that the X-ray structure of KcsA also corresponds to a closed state (Meuser et al. 1999).

Determination of ionization state

A further feature that is conserved between the two structures is the presence of rings of acidic sidechains at the extracellular mouth of the channel (Fig. 3C, D). Thus, in KcsA the mouth is surrounded by a ring of D80 sidechains. In the *Shaker* model there is a corresponding ring of D447 sidechains, plus an "outer" ring of D431 sidechains. In general, these acidic sidechains would be expected to generate a favourable electrostatic potential for cations in the vicinity of the mouth to the pore (Guidoni et al. 1999). However, there is a complication that has to be taken into account.

Previous studies on early models of the *Shaker* pore (Ranatunga et al. 1998) and, more recently, on KcsA (Ranatunga et al. 2001) have shown that the ionization state of the acidic sidechain rings at the channel mouth can differ somewhat from their standard, "model" values (i.e. from the pK_A values of the isolated amino acids in solution). Moreover, such perturbations of pK_A values may influence interactions between ions and the channel. Continuum electrostatics methods were used to evaluate the ionization states of sidechains in the *Shaker* pore model (see Methods). Most ionizable sidechains were found to be in their standard states at neutral pH even though their pK_A values were somewhat perturbed from the corresponding model pK_A values (Table 1). However, the Asp447 ring, located at the top of the selectivity filter, exhibits greatly altered pK_A values such that, on average, two of the four sidechains are expected to remain protonated at pH 7 (Fig. 4). This perturbation is dominated largely by unfavourable interactions with the nearby Asp431 ring and by the low dielectric surroundings of Asp447. Mutational data highlight both the Asp447 (Aiyar et al. 1996; Kirsch et al. 1995; Kürz et al. 1995; Liu et al. 1996; Lü and Miller 1995; Pascual et al. 1995; Ranganathan et al. 1996) and the Asp431 (Goldstein et al. 1994; Gross and MacKinnon 1996; Gross et al. 1994; Kürz et al. 1995; Lü and Miller 1995; MacKinnon and Miller 1989; MacKinnon and Yellen 1990; MacKinnon et al. 1990; Ranganathan et al. 1996; Yellen et al. 1991) rings as being of functional importance. The Asp431 ring affects permeation and is involved in the binding of extracellular toxins. The Asp447 ring affects selectivity and also helps to bind toxins. It is of interest to note that the equivalent ring of residues in KcsA also exhibits altered titration behaviour (Ranatunga et al. 2001), sharing its protons with a lower ring of Glu71 residues (which have no equivalent in *Shaker*). Thus, in both K^+ channels the density of negative charge in the extracellular mouth is somewhat less than might otherwise be expected because of the interactions of clusters of acidic sidechains.

Effect of ionization state on ion-pore-water interactions along the channel

To explore the functional consequences of altered ionization state, MD calculations were employed to calculate the potential energy of interaction (with protein and water) of a K^+ ion placed at 1 Å intervals along the pore axis. This was performed both using default ionization states (i.e. all acidic sidechains negatively charged and all

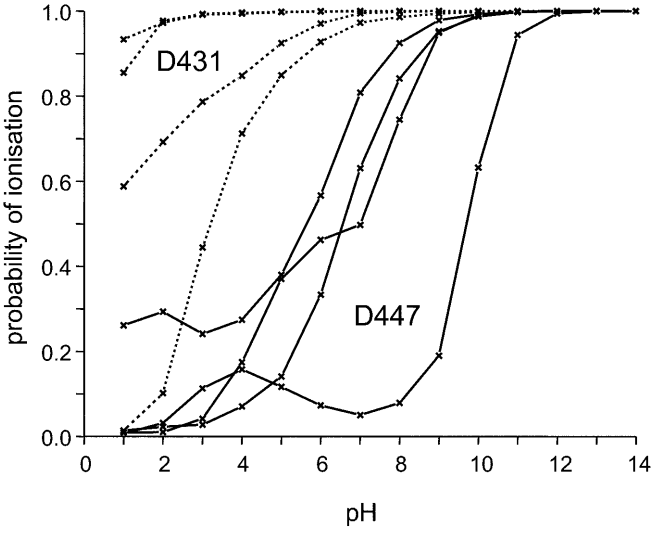

Fig. 4 Calculated titration curves for residues Asp431 (*dotted*) and Asp447 (*solid*) of the *Shaker* model

Table 1 pK_A values of ionizable sidechains in the *Shaker* model. The table shows the Born (solvation by dielectric environment) and back (solvation by the background of partial charges) energies, and the intrinsic and final (i.e. including interaction with other ionizable residues) pK_A values of ionizable residues in the *Shaker* pore homology model. The mean and standard deviations are presented for each ring of the sidechains

Ring	Model pK_A	Born energy (kcal mol^{-1})	Back energy (kcal mol^{-1})	Intrinsic pK_A	Final pK_A
Arg394	12.0	0.4 ± 0.2	0.6 ± 0.3	11.3 ± 0.3	11.9 ± 0.2
Glu395	4.4	–2.8 ± 1.0	2.4 ± 1.0	4.7 ± 1.3	4.6 ± 1.4
Glu418	4.4	–6.6 ± 0.2	13.1 ± 2.5	–0.3 ± 1.8	< 0.0
Glu422	4.4	–0.0 ± 0.0	0.0 ± 0.1	4.4 ± 0.1	4.7 ± 0.1
Lys427	10.4	2.2 ± 0.8	–4.3 ± 5.0	11.9 ± 3.2	13.5 ± 1.2
Asp431	4.0	–4.0 ± 0.9	3.2 ± 0.4	4.6 ± 0.9	0.8 ± 1.6
Asp447	4.0	–3.6 ± 0.3	4.7 ± 1.1	3.2 ± 0.6	7.2 ± 1.7
Lys456	10.4	6.0 ± 0.5	1.0 ± 0.7	5.3 ± 0.4	14.5 ± 0.0

basic sidechains positively charged) and using the calculated values (i.e. values derived from the calculated titration curves and assuming pH 7).

The sole difference between the default and pH 7 states is the protonation of two of the four Asp447 rings. The Asp 447 ring, when fully ionized, contributes a large well of ca. –110 kcal mol^{-1} to the ion-protein interaction near the top of the selectivity filter. On neutralization of half the ring, this well decreases in depth to only ca. −50 kcal mol^{-1}. The ring's effect extends over a large range (0–15 Å) through the selectivity filter and into the extracellular mouth.

The potential profile shows a large barrier (ca. 90 kcal mol^{-1}) to an ion at the intracellular end of the channel (Fig. 5A). This is largely due to the extreme constriction here (the valine of the PVP S6 motif discussed earlier constricts the pore), which increases the ion-water barrier (i.e. the ion is dehydrated), this dehydration not compensated for by any favourable ion-protein interactions (Fig. 5B). This supports our contention that this model corresponds to a closed channel.

Within the aqueous cavity, the profile drops back down to zero and then proceeds to drop further as the K^+ ion begins to sense the influence of the pore helix dipoles (Roux and MacKinnon 1999) and the oxygen atoms within the selectivity filter. The ion-water interaction is favourable within the cavity relative to in the filter, but is less favourable than in bulk water.

The selectivity filter

The structure of the selectivity filter in the *Shaker* model is shown in Fig. 6A. As in KcsA, the filter can be thought of as a number of "sites", each formed by two

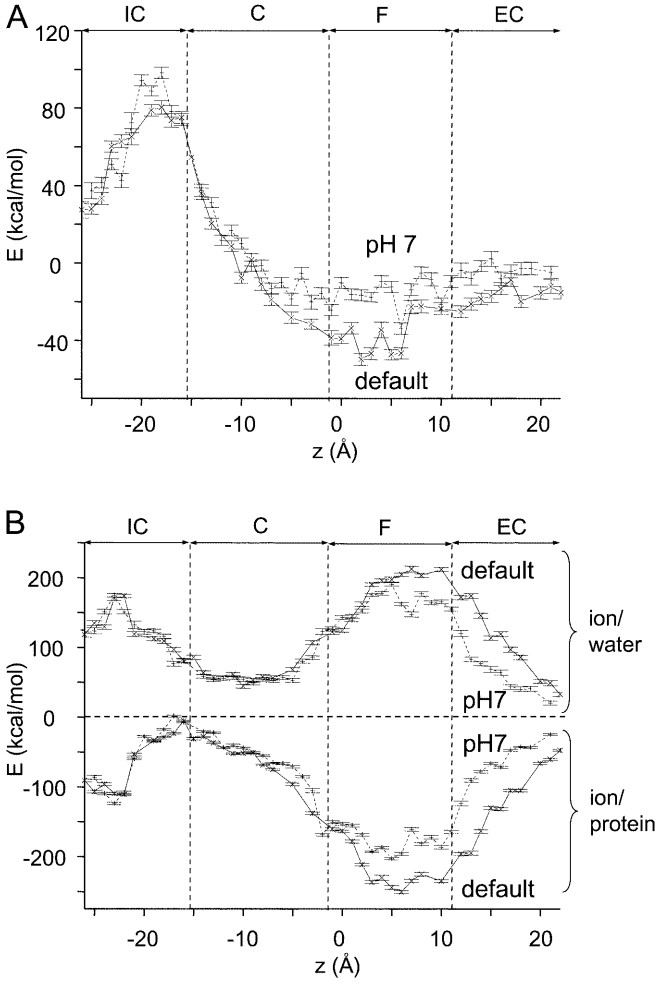

Fig. 5A, B Interaction potential energy profiles for translation of a single K^+ ion along the solvated *Shaker* pore homology model. **A** Potential energy profile for the interaction between a K^+ ion and (protein + water). "Default" indicates that all ionizable sidechains were assumed to be fully ionized; "pH 7" indicates that predicted ionization states at pH 7 based on the pK_A calculations were used. **B** Interaction potential energy profiles of a K^+ ion with water (*upper curves*) and with the protein (*lower curves*)

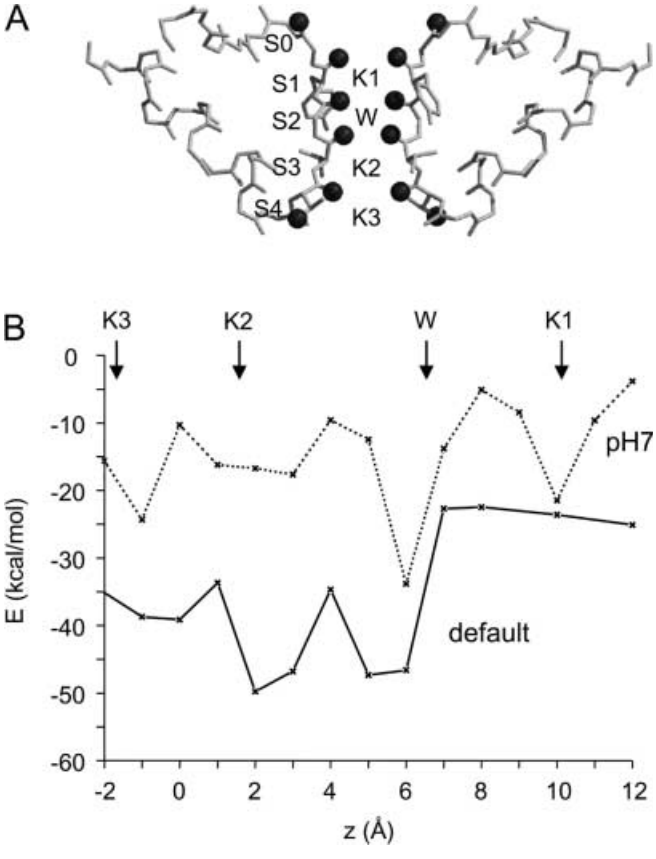

Fig. 6 **A** Structure of the *Shaker* model selectivity filter. For clarity, only two subunits are shown. The oxygen atoms that line the filter are shown as *grey spheres*. K1, W, K2, K3 indicate the approximate corresponding positions of the three K^+ ions plus water molecule observed in the KcsA structure. **B** Interaction energy profiles for a K^+ ion with (protein + water) interaction within the selectivity filter of the *Shaker* model. "Default" indicates that all ionizable sidechains were assumed to be fully ionized; "pH 7" indicates that predicted ionization states at pH 7 based on the pK_A calculations were used. The approximate locations of the ions and water molecule (as shown in **A**) are indicated by the *vertical arrows*

rings of four oxygen atoms. In the KcsA X-ray structure, sites S1, S2, S3 and S4 are occupied by, respectively, a K^+ ion, a water molecule, a K^+ ion and a K^+ ion. As the *Shaker* filter structure is very similar to that of KcsA, it is of interest to examine the ion interaction energy profiles in this region in a little more detail.

The profile within the selectivity filter region (Fig. 6B) is significantly different for the two ionization states as it is modulated by the protonation of residues in the Asp447 ring (as discussed). In the default state the potential energy (relative to an ion in "bulk" solvent) ranges from ca. –50 kcal mol^{-1} to ca. –20 kcal mol^{-1}, whereas it is around –20 kcal mol^{-1} throughout in the pH 7 state. It is evident that the potential wells for the "pH 7" ionization state are not as deep as for the "default" ionization state, and thus are more consistent with a high cation flux exhibited by the channel in its conductance value of 19 pS (Heginbotham and MacKinnon 1993; Tagliatela et al. 1994). Interestingly, a similar difference between the "default" and "pH 7" profiles is seen for KcsA (Ranatunga et al. 2001). Furthermore, it is encouraging to note that the wells in the "default" profile agree with the presumed positions of the ions and water molecule derived from the KcsA crystal structure.

Discussion

Biological implications

It is evident that a homology model of the pore domain of *Shaker* is convincing by a number of membrane protein structural criteria. It is therefore worth exploring further via simulation studies and related calculations. However, as the results described above indicate, there is a complication in such studies relating to the presence of a number of ionizable sidechains that may in turn influence the energetics of ion permeation.

A key feature of the *Shaker* pore domain model (a feature shared with KcsA and with other K^+ channel models) is the presence of a number of rings of ionizable sidechains around the extracellular mouth of the channel. In particular, two rings of acidic sidechains are present that might be expected to "steer" cations to/from the mouth of the channel. The members of the innermost ring of acidic sidechains (D447) are predicted to be incompletely ionized at pH 7. One consequence of this is to provide a more favourable (i.e. flatter) energy profile in the selectivity filter, consistent with a high rate of ion permeation. This is similar to recent results for KcsA (Ranatunga et al. 2001).

We note that calculation of the ionization state of a channel protein also provides a more realistic structure from which to start a MD simulation in order to better understand ion permeation (Sansom et al. 2000). However, ideally such simulations would be run such that the ionization state was updated frequently throughout the course of the simulations (Sandberg and Edholm 1997).

Critical assessment of methodology

Perhaps the main limitation of the current study is that only the central pore-forming domain of the *Shaker* K_v channel is included in the calculations. Thus the surrounding S1 to S4 helices are omitted, as are the extramembraneous domains and ancillary subunits (Biggin et al. 2000). It is conceivable that the omitted regions may alter the details of the pK_A calculations. However, as the principal factor suppressing the ionization of the D447 sidechains is their proximity to one another, the main results of the current study are unlikely to be changed.

A further limitation is that the current study is of a model of the pore domain of *Shaker* in a closed conformation of the channel. Recent experimental (Camino et al. 2000) and simulation (Kerr et al. 1996; Shrivastava et al. 2000) studies suggest that the S6 helix of K_v channels is capable of kinking in the region of the conserved Pro-Val-Pro sequence motif in the middle of this helix. Given that studies of KcsA locate the gate at the intracellular mouth of the channel (Perozo et al. 2000; Shrivastava and Sansom 2000), it seems likely that dynamic changes in the conformation of S6 may be associated with K_v channel activation. One approach to modelling an open conformation of a K_v channel may be to combine homology modelling with simulation-derived information on the flexibility of the Pro-Val-Pro hinge in the S6 helix (Tieleman et al. 2001b). Such an open-state model could then be analysed in a similar fashion to that used in the current study.

In terms of the MD simulations to look at ion potential profiles, their main limitations are that the protein is restrained and the simulations are short. In the absence of a more complete structure for a K_v channel, unrestrained simulations are not feasible. Longer simulations are probably not justifiable if restraints are used. In calculating the potential (rather than free energy) profile, only a first approximation at the ion permeation energetics is obtained. However, perhaps a more critical limitation is the use of a *single* K^+ ion in such calculations. Both experimental (Hille 1992) and simulation (Bernèche and Roux 2000; Capener et al. 2000; Guidoni et al. 1999, 2000; Shrivastava and Sansom 2000) studies indicate that the selectivity filter of a K channel can accommodate multiple K^+ ions, and thus future studies will need to calculate ion-channel interaction energies as a function of the locations of at least two ions.

A further limitation of the electrostatics calculations used in estimation of pK_A values is that they are based on an equilibrium assumption. Of course, this is only a first approximation to the situation of ion channels in a cell membrane and so future work will require treatment of the non-equilibrium state (Chen et al. 1997).

What are the main sources of error in the current calculations? Both of these are linked to the use of KcsA as a template for the *Shaker* channel. Firstly, as shown experimentally (Camino et al. 2000) and computationally

(Kerr et al. 1996; Sansom and Weinstein 2000; Shrivastava et al. 2000; Tieleman et al. 2001b), the S6 helix may be kinked in the vicinity of the Pro-Val-Pro motif. As discussed above, in some of the simulations a K^+ ion in the vicinity of the intracellular mouth of the pore experienced large energy fluctuations. This is exactly the region of the channel model whose geometry would be changed by a kink in the S6 helices. Secondly, errors in the pK_A calculations per se, for example due to small differences between different homology models from the same family, are likely to be substantially smaller than those due to assuming KcsA as a template. Thus, in order to substantially reduce error in both aspects of these calculations, we are currently pursuing methods to include, for example, the possibility of an S6 helix kink in second-generation *Shaker* pore homology models, based upon improved knowledge of the possible conformations of the S6 helix from longer simulations of the isolated helix than those described elsewhere (e.g. Shrivastava et al. 2000).

Finally, a more biological consideration. In this and an earlier study (Ranatunga et al. 2001) we have shown that rings of acidic sidechains close to the mouth of the channel play an important role in determining the energetic profile of *Shaker* and KcsA, respectively. It will be important to extend such studies to homology models of a number of different K^+ channels in order to see to what extent this property is important for K^+ channels in general.

Acknowledgements This work was supported by grants from the Wellcome Trust. R.J.L. is supported by a MRC studentship.

References

Adcock C, Smith GR, Sansom MSP (1998) Electrostatics and the selectivity of ligand-gated ion channels. Biophys J 75:1211–1222

Adcock C, Smith GR, Sansom MSP (2000) The nicotinic acetylcholine receptor: from molecular model to single channel conductance. Eur Biophys J 29:29–37

Aiyar J, Rizzi JP, Gutman GA, Chandy KG (1996) The signature sequence of voltage-gated potassium channels projects into the external vestibule. J Biol Chem 271:31013–31016

Allen TW, Bliznyuk A, Rendell AP, Kuyucak S, Chung SH (2000) The potassium channel: structure, selectivity and diffusion. J Chem Phys 112:8191–8204

Åqvist J, Luzhkov V (2000) Ion permeation mechanism of the potassium channel. Nature 404:881–884

Barton GJ (1990) Protein multiple sequence alignment and flexible pattern matching. Methods Enzymol 183:403–428

Bashford D, Karplus M (1990) pKa's of ionisable groups in proteins: atomic detail from a continuum electrostatic model. Biochemistry 29:10219–10225

Bernèche S, Roux B (2000) Molecular dynamics of the KcsA K^+ channel in a bilayer membrane. Biophys J 78:2900–2917

Biggin PC, Roosild T, Choe S (2000) Potassium channel structure: domain by domain. Curr Opin Struct Biol 10:456–461

Biggin PC, Smith GR, Shrivastava IH, Choe S, Sansom MSP (2001) Potassium and sodium ions in a potassium channel studied by molecular dynamics simulations. Biochim Biophys Acta (in press)

Brooks BR, Bruccoleri RE, Olafson BD, States DJ, Swaminathan S, Karplus M (1983) CHARMM: a program for macromolecular energy, minimisation, and dynamics calculations. J Comput Chem 4:187–217

Camino DD, Holmgren M, Liu Y, Yellen G (2000) Blocker protection in the pore of a voltage-gated K^+ channel and its structural implications. Nature 403:321–325

Capener CE, Shrivastava IH, Ranatunga KM, Forrest LR, Smith GR, Sansom MSP (2000) Homology modelling and molecular dynamics simulation studies of an inward rectifier potassium channel. Biophys J 78:2929–2942

Chen D, Lear J, Eisenberg B (1997) Permeation through an open channel: Poisson-Nernst-Planck theory of a synthetic ionic channel. Biophys J 72:97–116

Cserzo M, Wallin E, Simon I, von Heijne G, Elofsson A (1997) Prediction of transmembrane alpha-helices in prokaryotic membrane proteins: the dense alignment surface method. Protein Eng 10:673–676

Davis ME, Madura JD, Luty BA, McCammon JA (1991) Electrostatics and diffusion of molecules in solution: simulations with the University of Houston Brownian dynamics program. Comput Phys Commun 62:187–197

Donnelly D, Overington JP, Ruffle SV, Nugent JHA, Blundell TL (1993) Modelling α-helical transmembrane domains: the calculation and use of substitution tables for lipid-facing residues. Protein Sci 2:55–70

Doyle DA, Cabral JM, Pfuetzner RA, Kuo A, Gulbis JM, Cohen SL, Cahit BT, MacKinnon R (1998) The structure of the potassium channel: molecular basis of K^+ conduction and selectivity. Science 280:69–77

Durell SR, Hao YL, Guy HR (1998) Structural models of the transmembrane region of voltage-gated and other K^+ channels in open, closed, and inactivated conformations. J Struct Biol 121:263–284

Elinder F, Århem P (1999) Role of individual surface charges of voltage-gated K channels. Biophys J 77:1358–1362

Frankenhaeuser B, Hodgkin AL (1957) The action of calcium on the electrical properties of squid axons. J Physiol (Lond) 137:218–244

Goldstein SAN, Pheasant DJ, Miller C (1994) The charybdotoxin receptor of a *Shaker* K^+ channel: peptide and channel residues mediating molecular recognition. Neuron 12:1377–1388

Gross A, MacKinnon R (1996) Agitoxin footprinting the *Shaker* potassium channel pore. Neuron 16:399–406

Gross A, Abramson T, MacKinnon R (1994) Transfer of the scorpion toxin receptor to an insensitive potassium channel. Neuron 13:961–966

Guidoni L, Torre V, Carloni P (1999) Potassium and sodium binding in the outer mouth of the K^+ channel. Biochemistry 38:8599–8604

Guidoni L, Torre V, Carloni P (2000) Water and potassium dynamics in the KcsA K^+ channel. FEBS Lett 477:37–42

Heginbotham L, MacKinnon R (1993) Conduction properties of the cloned *Shaker* K^+ channel. Biophys J 65:2089–2096

Heginbotham L, LeMasurier M, Kolmakova-Partensky L, Miller C (1999) Single *Streptomyces lividans* K^+ channels: functional asymmetries and sidedness of proton activation. J Gen Physiol 114:551–559

Heijne G von (1992) Membrane protein structure prediction. Hydrophobicity analysis and the positive inside rule. J Mol Biol 225:487–494

Hille B (1992) Ionic channels of excitable membranes, 2nd edn. Sinauer Associates, Sunderland, Mass

Kerr ID, Sansom MSP (1997) The pore-lining region of *Shaker* voltage-gated potassium channels: comparison of β-barrel and α-helix bundle models. Biophys J 73:581–602

Kerr ID, Son HS, Sankararamakrishnan R, Sansom MSP (1996) Molecular dynamics simulations of isolated transmembrane helices of potassium channels. Biopolymers 39:503–515

Kirsch GE, Pascual JM, Shieh C-C (1995) Functional role of a conserved asparagine in the external mouth of voltage-gated potassium channels. Biophys J 68:1804–1813

Komiya H, Yeates TO, Rees DC, Allen JP, Feher G (1987) Structure of the reaction centre from *Rhodobacter sphaeroides*

R-26 and 2.4.1: symmetry relations and sequence comparisons. Proc Natl Acad Sci USA 85:9012–9016
Kraulis PJ (1991) MOLSCRIPT: a program to produce both detailed and schematic plots of protein structures. J Appl Crystallogr 24:946–950
Kürz LL, Zühlke RD, Zhang H-J, Joho RH (1995) Side-chain accessibilities in the pore of a K^+ channel probed by sulphydryl-specific reagents after cysteine-scanning mutagenesis. Biophys J 68:900–905
Laskowski RA, Macarthur MW, Moss DS, Thornton JM (1993) PROCHECK – a program to check the stereochemical quality of protein structures. J Appl Crystallogr 26:283–291
Liu Y, Jurman ME, Yellen G (1996) Dynamic rearrangement of the outer mouth of a K^+ channel during gating. Neuron 16:859–867
Lü Q, Miller C (1995) Silver as a probe of pore-forming residues in a potassium channel. Science 268:304–307
MacKinnon R, Miller C (1989) Mutant potassium channel with altered binding of charybdotoxin, a pore-blocking peptide inhibitor. Science 245:1382–1385
MacKinnon R, Yellen G (1990) Mutations affecting TEA blockade and ion permeation in voltage activated K^+ channels. Science 250:276–279
MacKinnon R, Heginbotham L, Abramson T (1990) Mapping the receptor site for charybdotoxin, a pore-blocking potassium channel inhibitor. Neuron 5:767–771
MacKinnon R, Cohen SL, Kuo A, Lee A, Chait BT (1998) Structural conservation in prokaryotic and eukaryotic potassium channels. Science 280:106–109
Merritt EA, Bacon DJ (1997) Raster3D: photorealistic molecular graphics. Methods Enzymol 277:505–524
Meuser D, Splitt H, Wagner R, Schrempf H (1999) Exploring the open pore of the potassium channel from *Steptomyces lividans*. FEBS Lett 462:447–452
Momany FA, Rone R (1992) Validation of the general purpose QUANTA 3.2/CHARMm forcefield. J Comput Chem 13:888–900
Pascual JM, Shieh C-C, Kirsch GE, Brown AM (1995) Multiple residues specify external tetraethylammonium blockade in voltage-gated potassium channels. Biophys J 69:428–434
Perozo E, Cortes DM, Cuello LG (1999) Structural rearrangements underlying K^+-channel activation gating. Science 285:73–78
Perozo E, Liu YS, Smopornpisut P, Cortes DM, Cuello LG (2000) A structural perspective of activation gating in K^+ channels. J Gen Physiol 116:5a
Persson B, Argos P (1994) Prediction of transmembrane segments utilizing multiple sequence alignments. J Mol Biol 237:182–192
Persson B, Argos P (1997) Prediction of membrane protein topology utilizing multiple sequence alignments. J Protein Chem 16:453–457
Plugge B, Gazzarrini S, Nelson M, Cerana R, Van Etten JL, Derst C, DiFrancesco D, Moroni A, Thie G (2000) A potassium channel protein encoded by chlorella virus PBCV-1. Science 287:1641–1644
Ranatunga KM, Adcock C, Kerr ID, Smith GR, Sansom MSP (1999) Ion channels of biological membranes: prediction of single channel conductance. Theor Chem Acc 101:97–102
Ranatunga KM, Shrivastava IH, Smith GR, Sansom MSP (2001) Sidechain ionisation states in a potassium channel. Biophys J 80:1210–1219
Ranatunga KR, Kerr ID, Adcock C, Smith GR, Sansom MSP (1998) Protein-water-ion interactions in a model of the pore domain of a potassium channel: a simulation study. Biochim Biophys Acta 1370:1–7
Ranganathan R, Lewis JH, MacKinnon R (1996) Spatial localization of the K^+ channel selectivity filter by mutant cycle-based structure analysis. Neuron 16:131–139
Rodriguez R, Chinea G, Lopez N, Pons T, Vriend G (1998) Homology modelling, model and software evaluation: three related sources. CABIOS 14:523–528
Rost B, Casadio R, Fariselli P, Sander C (1995) Prediction of helical transmembrane segments at 95% accuracy. Protein Sci 4:521–533
Rost B, Fariselli P, Casadio R (1996) Topology prediction for helical transmembrane proteins at 86% accuracy. Protein Sci 5:1704–1718
Roux B, MacKinnon R (1999) The cavity and pore helices in the KcsA K^+ channel: electrostatic stabilization of monovalent cations. Science 285:100–102
Sanchez R, Sali A (1997) Advances in comparative protein-structure modelling. Curr Opin Struct Biol 7:206–214
Sandberg L, Edholm O (1997) pK_a calculations along a bacteriorhodopsin molecular dynamics trajectory. Biophys Chem 65:189–204
Sansom MSP, Weinstein H (2000) Hinges, swivels and switches: the role of prolines in signalling via transmembrane α-helices. Trends Pharm Sci 21:445–451
Sansom MSP, Shrivastava IH, Ranatunga KM, Smith GR (2000) Simulations of ion channels – watching ions and water move. Trends Biochem Sci 25:368–374
Schachtman DP (2000) Molecular insights into the structure and function of plant K^+ transport mechanisms. Biochim Biophys Acta 1465:127–139
Schrempf H, Schmidt O, Kummerlein R, Hinnah S, Muller D, Betzler M, Steinkamp T, Wagner R (1995) A prokaryotic potassium-ion channel with 2 predicted transmembrane segments from *Steptomyces lividans*. EMBO J 14:5170–5178
Shrivastava IH, Sansom MSP (2000) Simulations of ion permeation through a potassium channel: molecular dynamics of KcsA in a phospholipid bilayer. Biophys J 78:557–570
Shrivastava IH, Capener C, Forrest LR, Sansom MSP (2000) Structure and dynamics of K^+ channel pore-lining helices: a comparative simulation study. Biophys J 78:79–92
Smith GR, Sansom MSP (1997) Molecular dynamics study of water and Na^+ ions in models of the pore region of the nicotinic acetylcholine receptor. Biophys J 73:1364–1381
Tagliatela M, Champagne MS, Drewe JA, Brown AM (1994) Comparison of H5, S6 and H5-S6 exchanges on pore properties of voltage-dependent K^+ channels. J Biol Chem 269:13867–13873
Tempel BL, Papazian DM, Schwarz TL, Jan YN, Jan LY (1987) Sequence of a probable potassium channel component encoded at *Shaker* locus of *Drosophila*. Science 237:770–775
Thompson GA, Leyland ML, Ashmole I, Sutcliffe MJ, Stanfield PR (2000) Residues beyond the selectivity filter of the K^+ channel Kir2.1 regulate permeation and block by external Rb^+ and Cs^+. J Physiol (Lond) 526:231–240
Tieleman DP, Breed J, Berendsen HJC, Sansom MSP (1998) Alamethicin channels in a membrane: molecular dynamics simulations. Faraday Discuss 111:209–223
Tieleman DP, Biggin PC, Smith GR, Sansom MSP (2001a) Simulation approaches to ion channel structure-function relationships. Q Rev Biophys (in press)
Tieleman DP, Shrivastava IH, Ulmschneider MB, Sansom MSP (2001b) Proline-induced hinges in transmembrane helices: possible roles in ion channel gating. Proteins Struct Funct Genet (in press)
Vriend G (1990) A molecular modelling and drug design program. J Mol Graphics 8:52–56
Yang A, Gunner MR, Sampogna R, Sharp K, Honig B (1993) On the calculation of pK_As in proteins. Proteins Struct Funct Genet 15:252–265
Yau WM, Wimley WC, Gawrisch K, White SH (1998) The preference of tryptophan for membrane interfaces. Biochemistry 37:14713–14718
Yellen G, Jurman ME, Abramson T, MacKinnon R (1991) Mutations affecting internal TEA blockade identify the probable pore forming region of a K^+ channel. Science 251:939–942